

X-Ray Reflection Phases and Dynamical Diffraction Effects

Shih-Lin Chang

Department of Physics, National Tsing Hua University,
Hsinchu, Taiwan 300, R. O.C.

(Received October 24, 1997)

The relationship between X-ray reflection phases and dynamical diffraction effects is briefly reviewed. Discussion is also given to x-ray phase determination using coherent dynamical interaction in 2-beam and 3-beam diffractions.

PACS. 61.10.Dp – Theories of diffraction and scattering.

PACS. 61.10.Lx – Experimental diffraction and scattering techniques.

I. Introduction

X-ray diffraction from crystals is usually considered as an interference phenomenon of electromagnetic waves with a three-dimensional periodic array of atoms in the angstrom scale. The amplitudes and phases of the diffracted x-rays are the important quantities to be determined or measured in relation to the interaction of the EM waves with the crystal lattice and to the arrangement of the atoms in the crystal. In x-ray diffraction experiments, the amplitude of a diffracted wave can be easily determined from intensity measurements. However, to measure the phase of an x-ray reflection is not always attainable. This fact constitutes the well-known x-ray phase problem in diffraction physics and x-ray crystallography [1]. Like in optics, x-ray reflection phase should, in principle, be determined from interference experiments, where maintaining temporal and spatial coherence of x-rays in crystals is a prime requirement.

It is a tradition in x-ray crystallography to consider a crystal to be composed of many tiny perfect crystal blocks, misoriented with one another. The average misorientation, the so-called mosaic spread, is a measure of whether the crystal is perfect or imperfect. X-ray diffraction from a crystal is therefore a result of the interaction between inter-diffractions among the various crystal blocks and intra-diffractions within a crystal block. The interaction can be either coherent or incoherent depending on the crystal perfection. If the crystal is perfect, namely with a negligibly small mosaic spread, then the resultant coherent interaction between the inter- and intra-diffractions, which maintain the coherent phase relationship among the diffracted x-ray waves from the various crystal blocks, leads to observable “dynamical” effects. Theories developed based on this assumption have been called “dynamical theories”, in contrast to the “kinematical” theories which deal with incoherent interactions in imperfect crystals.

In this article we briefly review the dynamical theory and present analyses of dynamical diffraction effects in relation to phases of diffracted waves. Investigation in solving the x-ray phase problem using dynamical effects is also discussed.

II. Dynamical theory of x-ray diffraction

The dynamical nature of x-ray diffraction was first considered by Ewald [2] and modified by von Laue [3]. For simplicity, we follow Laue's dynamical treatment, where the crystal is considered as a complex dielectric medium. X-ray diffraction from the crystal is then described by Maxwell's equations, whose solutions are the Bloch functions expressed as

$$D(\vec{r}, t) = \sum_{\vec{G}} \bar{D}_{\vec{G}} \exp(i\omega t - 2\pi i \vec{K}_{\vec{G}} \cdot \vec{r}) \quad (1)$$

for electric displacements, where $\vec{K}_{\vec{G}}$ is the wavevector of the G-reflection satisfying Bragg's law, i.e.

$$\vec{K}_{\vec{G}} = \vec{K}_0 + \vec{g}_{\vec{G}} \quad (2)$$

for every G-reflection involved.

Let the electric susceptibility, $\chi/4\pi$, be expressed as a Fourier series:

$$\chi = \sum_{\vec{G}} \chi_{\vec{G}} \exp[-2\pi i(\vec{g}_{\vec{G}} \cdot \vec{r})] \quad (3)$$

where

$$\chi_{\vec{G}} = -\frac{r_e \lambda^2}{\pi V} F_{\vec{G}} \quad (4)$$

$F_{\vec{G}}$ is the structure-factor of the G-reflection, r_e is the classic radius of the electron (i.e. $r_e = \frac{e^2}{mc^2}$), λ the x-ray wavelength and V the volume of a crystal unit cell.

By substituting the Bloch functions and the electric susceptibility into Maxwell's equations, the Fourier components satisfy the so-called fundamental equation of wavefield given below:

$$\frac{K_{\vec{G}}^2 - k^2}{K_{\vec{G}}^2} \bar{D}_{\vec{G}} = \sum_L \chi_{\vec{G}-L} \bar{D}_{L(\perp \vec{K}_{\vec{G}})}, \quad (5)$$

where $D_{L(\perp \vec{K}_{\vec{G}})}$ represents the vector component of D_L perpendicular to the wavevector $\vec{K}_{\vec{G}}$ and $k = 1/\lambda$.

Employing the approximation $\vec{D} \cong \vec{E}$ at x-ray frequencies [3] and considering the polarization of x-rays, the fundamental equation can be written in the following matrix form

$$\Phi[\vec{E}] = 0$$

where \vec{E} is a column vector, expressed horizontally as $\vec{E} = [E_{\sigma 0} E_{\pi 0} E_{\sigma G_1} E_{\pi G_2} \dots E_{\sigma G_{N-1}} E_{\pi G_{N-1}}]$, and Φ is a $(2N \times 2N)$ complex matrix, with the diagonal terms equal to $\Phi(i, i) = \chi_0 - 2\epsilon_i$ and the off-diagonal terms $\Phi(i, j) = \chi_{i-j} p_{i-j}$ with $2\epsilon_i = (K_{\vec{G}_i}^2 - k^2)/k$. N is the

number of Bragg reflections involved and σ and π are the polarization unit vectors perpendicular to and lying in the plane of incidence, respectively. The polarization factor p_{i-j} is the product of the corresponding polarization unit vectors. 2ϵ 's are the eigenvalues which can be determined from the dispersion equation $\det [\Phi] = 0$ for non-trivial solutions for I , where \det stands for determinant. The real parts of 2ϵ 's describe the dispersion relation between the wavevectors and the crystal angular settings, while the imaginary parts yield the absorption. The fundamental equation gives also the eigenvectors, i.e., the ratios of the wavefield amplitudes among the diffracted beams. Their absolute amplitudes can be determined from the boundary conditions usually adopted in electromagnetism. Hence, the diffracted intensities can be calculated accordingly.

III. Dynamical effects versus reflection phases

III-1. Two-beam transmission case

When the diffraction involves an incident beam O and a transmitted reflected beam G and both beams O and G transmit through a crystal slab, the dispersion surface is a hyperbolic surface (Fig. 1). According to the dynamical theory [4], there are two modes of wave-propagation for each polarization. As shown in Fig. 1, branches 1 and 4 of the dispersion curves are associated with the σ polarization and branches 2 and 3 are associated with the π polarization. The relative phases of E_G with respect to E_O of modes 1 and 2 are 180° , while those of modes 3 and 4 are 0° , respectively. This phase difference among the various modes leads to differences in forming standing waves inside the crystal when the O waves and G waves are superimposed. For example, the sum of $E_O(1)$ and $E_G(1)$ forms a standing wave with its nodes at the diffracting planes, while $E_O(4) + E_G(4)$ has antinodes at the atomic planes. Therefore, mode 1 is low absorbing compared to the highly absorbing mode 4. When the crystal becomes very thick, for example, μ (linear

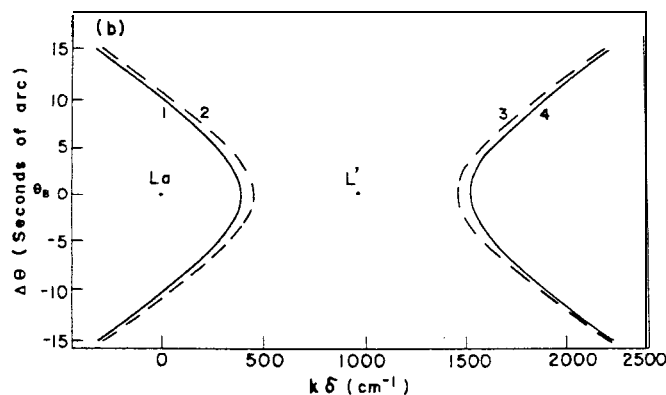


FIG. 1. Section of the dispersion surface in the plane of incidence of a 2-beam (O , G) x-ray diffraction. La and L' are the Laue point and the Lorentz point. $LaO = LaG = k$ and $L'O = L'G = k(1 + \chi_0/2)$. The ordinate $\Delta\theta$ is the angular deviation from the exact Bragg angle θ_B and the abscissa $k\delta$ is the resonance defect defining the location of wave-points.

absorption coefficient) $\times T$ (crystal thickness) > 10 , anomalous transmission takes place, because only the in-phase low absorbing mode survives, which contributes to the transmitted intensity. This is the well-known Borrmann effect [7].

111-2. Two-beam reflection case

When the reflecting atomic planes are parallel to the crystal surface, the diffraction is of Bragg-type (or reflection type) for the reflected beam \mathbf{G} and the transmitted beam 0 lie in the opposite side of the crystal. In this case, mode 1 and mode 4 are still out of phase. If we calculate the wavefield intensity of mode j , defined as $|E_O(j) + E_G(j)|^2$ (i.e., the intensity of the standing wave), for $G_e(111)$ reflection of $CuK\alpha_1$ radiation ($\lambda = 1.540562\text{\AA}$), we will always obtain the calculated intensity distribution versus the angular deviation $\Delta\theta$ from the exact Bragg angle θ_B , as shown in Fig. 2a. If the crystal is doped with As impurity atoms, and if the incident photon energy is greater than the K absorption edge of arsenic, then the measured fluorescence yield of As excited by the x-ray standing wave while varying $\Delta\theta$ shows the intensity asymmetry given in Fig. 2a, for substitutional arsenic atoms in the Ge lattice. Otherwise, the reversed asymmetry shown in Fig. 2b appears for interstitial arsenic atoms [8]. It should be noted that in the two-beam cases discussed, the diffracted intensity I_G provides no phase information about the structure factor F_G , since $I_G \propto |F_G|^2$. This is however not the case for the standing-wave excited fluorescence, because the electron density wave of the host crystal provides a reference for the x-ray fluorescence from the impurity atoms.

111-3. Three-beam diffraction

The dispersion surface of a 2-beam diffraction is a hyperbolic surface shown in Fig. 1. For a 3-beam (0, G, L) diffraction, due to the presence of the \mathbf{L} reflection, additional sheet appears in between the hyperbolic dispersion surface (Fig. 3). According to the dynamical theory, whether the additional sheet, branch 3, lies closer to branch 1 or to branch 2, depends on the phase δ_3 of the structure-factor triplet $F_{-G}F_LF_{G-L}$. If $\delta_3 \cong 0^\circ$, branch 3 is closer to branch 1, otherwise, branch 3 is closer to branch 2 for $\delta_3 = 180^\circ$ [9]. According to Ewald [2], the closer the dispersion branches, the stronger the diffracted intensity. Therefore, asymmetry of diffracted intensity distributions is expected. Indeed, the 3-beam diffraction intensity $I_G(\phi)$ versus the azimuthal angle ϕ around the reciprocal lattice vector \vec{g} of the G-reflection shows experimentally similar asymmetry as the fluorescence profiles given in Fig. 2. Namely, for $\delta_3 = 0^\circ$, the intensity I_G first decreases for lower ϕ angles then increases for higher ϕ angles, and vice versa for $\delta_3 = 180^\circ$ [10,11]. For $\delta_3 = \pm 90^\circ$, branch 3 of the dispersion surface lies at the Lorentz point L' (Fig. 3). It seems difficult to distinguish $+90^\circ$ from -90° . Fortunately, x-ray diffraction is an excitation process which is governed by the excitation function $\frac{1}{1+iA}$. Namely an additional phase varying from 0° to 180° takes place when the crystal is excited from 1-beam case (no diffraction) to 2-beam case. This phase difference together with the triplet phase δ_3 could eventually differentiate $\delta_3 = 90^\circ$ from -90° . The corresponding intensity profiles $I_G(\phi)$ are schematically shown in Fig. 4. From this qualitative analysis, x-ray reflection phases can be determined unambiguously [12].

Recent progress along this line has shown success in quantitative determination of phases of x-ray reflections from crystals of organic molecules and macromolecules [13,14].

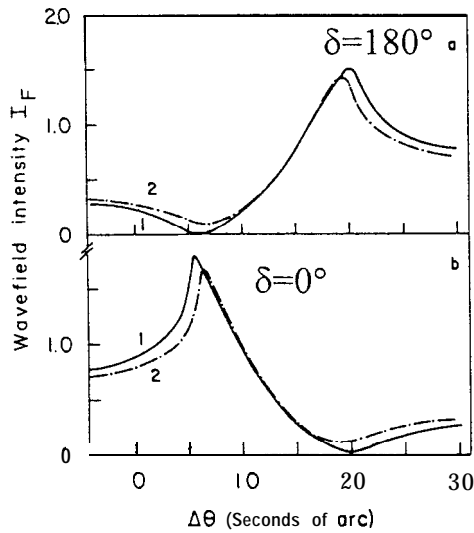


FIG. 2. Calculated intensity distributions of the x-ray wavefields, I_F , versus $\Delta\theta$, of the Ge reflection and $CuK\alpha_1$ radiation for (a) the phase δ of F(111) equal to 180° and (b) $\delta = 0^\circ$ for two permitted modes in a reflection geometry.

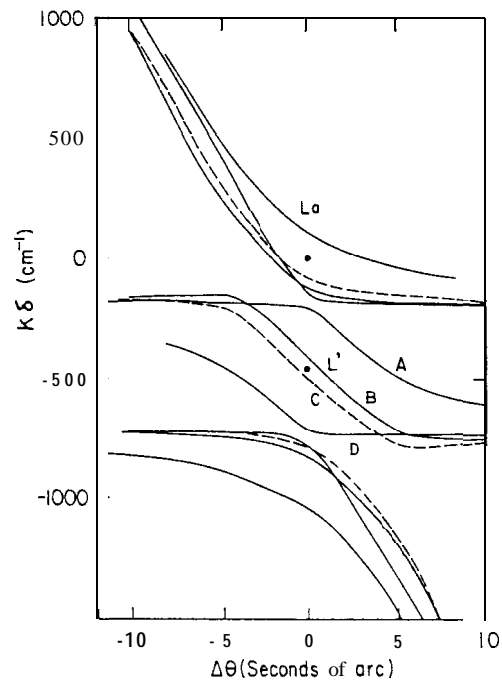


FIG. 3. Section of the dispersion surfaces A, B, C, and D in the plane of incidence of the G-reflection for a 3-beam (0, G, L) diffraction with $\delta_3 = 0^\circ$, $+90^\circ$, -90° , and 180° , respectively. La is the 3-beam Laue points and L' the 3-beam Lorentz point. (Only branches 3 are labeled by A, B, C, and D for the corresponding δ s.)

IV. Discussions and conclusions

In this paper we have discussed the relationship between dynamical diffraction effects and x-ray reflection phases. All the dynamical effects observed so far have been closely linked to the phases of crystal internal normal modes of wave-propagation, namely related to the phases of the structure-factors involved. Although these dynamical effects have usually been detected in x-ray diffraction from perfect crystals, they are still observable in real crystals, for then x-ray diffraction from the tiny perfect crystal blocks in real crystals is yet dynamical. This fact guarantees the success in phase determination of macromolecular crystals using 3-beam x-ray diffraction. By the same token, the dynamical effects just reviewed and discussed can, in principle, be applied to two-dimensional structures, namely to solve the x-ray phase problem for 2-d crystals. As a first step towards this goal, dynamical effects of surface in-plane reflections of a crystal need to be investigated. Since surface in-plane reflection usually involves grazing incidence geometry, the so-called n-beam GIXD,

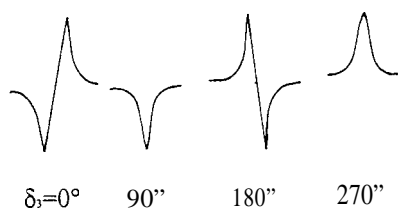


FIG. 4. Schematic representation of 3-beam intensity profiles $I_G(\phi)$ versus δ_3 .

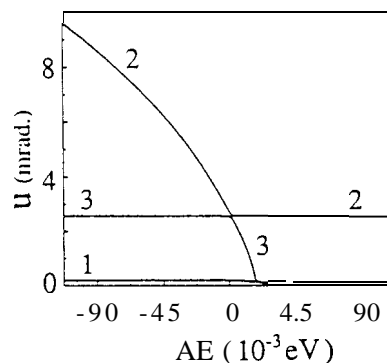


FIG. 5. Dispersion relation, $u = K_z^r/k$ vs. AE , at the critical angle of total reflection, 0.18° , for the 3-beam, (000) (440) (404), GIXD of silicon with $\delta_3 = 0^\circ$. K_z^r is the real part of the normal component of the wavevector \vec{K} and $k = 1/\lambda$ ($AE = E - E_M$, $E_M = 7.456$ keV.).

grazing incidence x-ray diffraction technique, is ideal for this type of investigation. For the phase determination of this kind, three-beam GIXD ($n = 3$) has to be employed.

For a three-beam GIXD, involving three surface in-plane reflections, three reciprocal lattice points, say 0 , G , and L , must not only be simultaneously placed on the surface of the Ewald sphere, but also lie in the equatorial plane of the sphere to ensure the diffracted beams being along the crystal surface. Since the radius of the equatorial circle circumscribing the three reciprocal lattice points is equal to $1/\lambda$ and depends on the reciprocal lattice vectors \vec{g} and \vec{l} , there is only a fixed wavelength (or photon energy) with which this particular 3-beam GIXD can take place. Because of the grazing incidence geometry, the ϕ -rotation around the \vec{g} vector cannot be used to guarantee that both the G and L reflections are still surface sensitive. Hence, the coherent dynamical interaction among the reflections involved may not provide enough phase information about the involved structure-factor triplets because of the geometry constraint. An alternative of achieving the ϕ -scan is to vary the wavelength, namely, to perform a photon-energy scan. At a specific λ_M (or the energy E_M), a 3-beam GIXD occurs. As an example, we consider the 3-beam, (000)(440)(404), GIXD of silicon. The dynamical effects of this 3-beam case can be well revealed from the dispersion surface of the wavevectors versus energies shown in Fig. 5. As can be seen, the dispersion relation representing the dynamical situation of the photon energy scan across E_M is similar to the dispersion relation shown in Fig. 3 of the angular position versus wavevector (momentum). According to the previous discussion given in Section 3, the closer the dispersion branches, the stronger the diffracted intensity. In Fig. 5, branch 3 is closer to branch 2 near $AE = 0$, the interaction between the normal modes 2 and 3 dominates, which should lead to the

intensity asymmetry as shown in Fig. 4a for $\delta_3 = 0^\circ$. This predicted intensity versus photon energies has recently been observed using the SRRC synchrotron radiation source. Details about the experiments will be reported elsewhere [15]. From this observation, the phase of the structure-factor triplet, $F(-4 \ 0 \ 0) F(4 \ 0 \ 4) F(04 \ -4)$ is determined to be 0° .

The author is indebted to the National Science Council for financial support during the course of this study.

References

- [1] See, for example, H. A. Hauptman, *Phys. Today* (November) 24, (1989).
- [2] P. P. Ewald, *Ann. Phys. (Leipzig)* 49, 1, 117 (1916); 54, 519 (1917).
- [3] M. von Laue, *Ergebn. Exakten Naturwiss.* 10, **133** (1931).
- [4] B. W. Battermann and H. Cole, *Rev. Mod. Phys.* 36, 681 (1964).
- [5] Z. G. Pinsker, *Dynamical Scattering of X-rays in Crystals* (Springer-Verlag, Heidelberg, 1977).
- [6] See, for example, *X-Ray and Neutron Dynamical Diffraction: Theory and Application*, eds. A. Authier, S. Lagomarsino, and B. K. Tanner, NATO ASI Series (Plenum Press, New York 1996).
- [7] G. Borrmann, *Phys. Z.* 42, 157 (1941).
- [8] B. W. Battermann, *Phys. Rev. Lett.* 22, 703 (1969).
- [9] P. P. Ewald and Y. Heno, *Acta Crystallogr.* A24, 5 (1968).
- [10] S. L. Chang, *Phys. Rev. Lett.* 48, 163 (1982).
- [11] S. L. Chang, *Multiple Diffraction of X-rays in Crystals* (Springer-Verlag, Heidelberg, 1984).
- [12] For reviews, see S. L. Chang, *Crystallogr. Rev.* 1(2), 85 (1987); E. Weckert and K. Hummer, *Acta Crystallogr.* A53, 108 (1997).
- [13] K. Hummer, E. Weckert, and H. Bondza, *Acta Crystallogr.* A47, 60 (1991).
- [14] S. L. Chang, H. E. King, M. T. Huang, and Y. Gao, *Phys. Rev. Lett.* 67, 3113 (1991).
- [15] S. L. Chang, Y. S. Huang, C. S. Chao, M. T. Tang, and Y. P. Stetsko, in preparation (1997).